CONNECTING DOMAINS AND CONTRASTING SAMPLES: A LADDER FOR DOMAIN GENERALIZATION

Anonymous authors
Paper under double-blind review

ABSTRACT

Distribution shifts between training and testing datasets, contrary to classical machine learning assumptions, frequently occur in practice and impede model generalization performance. Studies on domain generalization (DG) thereby arise, aiming to predict the label on unseen target domain data by only using data from source domains. In the meanwhile, the contrastive learning (CL) technique, which prevails in self-supervised pre-training, can align different augmentation of samples to obtain invariant representation. It is intuitive to consider the class-separated representations learned in CL are able to improve domain generalization, while the reality is quite the opposite: people observe directly applying CL deteriorates the performance. We analyze the phenomenon with the CL theory and discover the lack of intra-class connectivity in the DG setting causes the deficiency. Thus we propose domain-connecting contrastive learning (DCCL) to enhance the conceptual connectivity across domains and obtain generalizable representations for DG. Specifically, more aggressive data augmentation and cross-domain positive samples are introduced into self-contrastive learning to improve intra-class connectivity. Furthermore, to better embed the unseen test domains, we propose model anchoring to exploit the intra-class connectivity in pre-trained representations and complement it with generative transformation loss. Extensive experiments on five standard DG benchmarks are provided. The results verify that DCCL outperforms state-of-the-art baselines even without domain supervision.

1 INTRODUCTION

Neural networks have achieved great progress in various vision applications, such as visual recognition (He et al., 2016), object detection (Tan et al., 2020), semantic segmentation (Cheng et al., 2021), pose estimation (Sun et al., 2019), etc. Despite the immense success, existing approaches for representation learning typically assume that training and testing data are independently sampled from the identical distribution. However, in real-world scenarios, this assumption does not necessarily hold. In image recognition, for example, distribution shifts w.r.t. geographic location (Beery et al., 2018) and image background (Fang et al., 2013) frequently occur and impede the generalization performance of models.

Accordingly, domain generalization (DG) (Gulrajani & Lopez-Paz, 2020) is widely studied to strengthen the transferability of deep learning models. Different from domain adaptation (DA) (You et al., 2019; Tzeng et al., 2017) where unlabeled or partially labeled data in target domains are available during training, in a DG task we can only resort to source domains. A natural idea for DG is to learn invariant representation across a variety of seen domains so as to benefit the classification of unobserved testing domain samples. As a powerful representation learning technique, contrastive learning (CL) (Chen et al., 2020) aims to obtain class-separated representations and has the potential for DG (Yao et al., 2022). In this paper, however, we observe that the widely deployed self-contrastive learning (SCL) (Chen et al., 2020; He et al., 2020; Grill et al., 2020), which aligns the augmentation of the same input, does not naturally fit the domain generalization setting: it implicitly assumes the capability to sample instances from the whole data distribution.

To bridge this gap, we propose domain-connecting contrastive learning (DCCL) to pursue transferable representations in DG, whose core insight comes from a novel understanding of CL attributing the success of CL to the intra-class representation connectivity (Wang et al., 2022b). Specifically, we first suggest two direct approaches to improve *intra-class connectivity* (to be fully explained at the beginning of Section 2) within CL: (i) applying more aggressive data augmentation and (ii) expanding the scope of positive samples from self-augmented outputs to the augmentation of same-class samples across domains. In addition to the direct approaches, we have an interesting observation that the pre-trained models, unlike the learned maps, indeed possess the desired intra-class connectivity: the intra-class samples of the training domains and the testing domains are scattered but well-connected. The encouraging observation motivates us to anchor learned maps to the pre-trained model and further complement it with a generative transformation loss for stronger intra-class connectivity. As a visual illustration, Figure 1 demonstrates the embeddings learned by regular Empirical Risk Minimization (ERM) and by the proposed DCCL. ERM embeds the data in a more scattered distribution, and many samples in the central region cannot be distinguished; on the other hand, DCCL can well cluster and separate inter-class samples regardless of the domains. It verifies the effectiveness of our proposed DCCL on connecting domains.

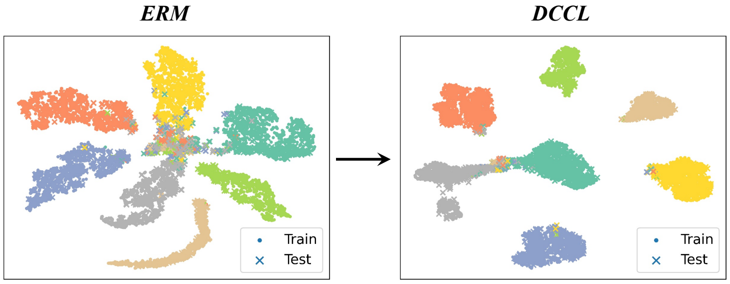

Figure 1: Visualization for ERM and DCCL on PACS. Intra-class points have the same colors, and two marker types differentiate the training and testing domains. Our proposed method better bridges the intra-class samples across domains than ERM.

Our contributions are summarized as follows:
(i) We analyze the failure of self-contrastive learning on DG and propose two effective strategies to improve intra-class connectivity within CL.
(ii) We propose to anchor learned maps to pre-trained models which possess the desired connectivity of training and testing domains. Generative transformation loss is further introduced to complement the alignment in between.
(iii) We conduct extensive experiments on five real-world DG benchmarks with various settings, demonstrating the effectiveness and rationality of DCCL.

2 Preliminaries

We first illustrate the core concept of the paper, *intra-class connectivity*. It refers to the intra-class data connectivity across different domains and resembles the connectivity in CL theory (Wang et al., 2022b), which depicts the preference that samples should not be isolated from other intra-class data of the same class [1]. In the remainder of this section, we introduce problem formulation and necessary preliminaries for contrastive learning in this section. A thorough review of related work on domain generalization and contrastive learning are deferred to Appendix B due to space limit.

2.1 Data in the domain generalization setting

Given N observations (from M domains), $\mathbf{X} = \{x_1, \ldots, x_N\} \subseteq \mathcal{X}$ is the collection of input features, $\mathbf{Y} = \{y_1, ..., y_N\} \subseteq \mathcal{Y}$ represents the prediction targets, and the whole dataset D_s is represented as $\{(x_i^m, y_i^m)_{i=1}^{N_m}\}_{m=1}^{M}$, where N_m is the number of samples ($\sum_{m=1}^{M} N_m = N$) in the domain d_m and x_i is re-indexed as x_i^m accordingly.

The goal of this paper is to train a generalizable classification model from partial domains in D_s, which has satisfactory performance even on the unseen domains in evaluation. We also follow the specific settings in Cha et al. (2021; 2022); Chen et al. (2022) where only the feature vector $x_i \in \mathbf{X}$ and the label $y_i \in \mathbf{Y}$ are observable, while the domain identifier $d_m \in \mathbf{D}$ cannot be explicitly utilized due to the expensive cost.

[1] An intuitive graph-based measure to assess the intra-class connectivity of a given model is discussed in Appendix A.4.

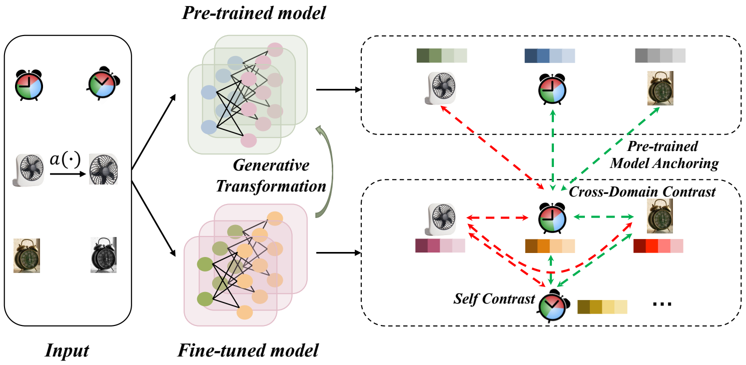

Figure 2: The overall framework of DCCL. The green dotted arrows indicate the two representations form a positive pair and the red ones connect the negative pairs. $a(\cdot)$ is an augmentation operation. Three key parts in DCCL are (i) cross-domain contrast to bridge the intra-class samples across domains; (ii) pre-trained model anchoring to further possess the intra-class connectivity; (iii) generative transformation to complement the pre-trained representation alignment.

2.2 Contrastive Learning

Contrastive Learning (CL) enforces the closeness of augmentation from the same input, compared to other inputs in the representation space. The main components of CL, as summarized in Chen et al. (2020); He et al. (2020), include: (i) data augmentation for contrastive views, (ii) a representation map f as the data encoder: $\mathcal{X} \rightarrow \mathbb{R}^d$, (iii) projection head $h(\cdot)$ for expressive representation, and (iv) contrastive loss for optimization. Given an instance from $\mathbf{X}$, we draw a positive pair x, x^+ by applying a random data augmentation $a \sim \mathcal{A}$, where $\mathcal{A}$ is the pre-specified distribution of random data augmentation maps. As a contrastive concept to positive samples, a negative pool $\mathcal{N}_x$ is the set of augmented samples randomly drawn from the whole dataset $\mathbf{X}$. To ease the construction of the CL loss, we denote $p(x)$ as the distribution of x, $p\left(x, x^+\right)$ as the corresponding joint distribution of the positive pairs, and $p_n(x_i^-)$ ("n" is shorthand for "negative") as the distribution for $x_i^- \in \mathcal{N}_x$, which are all independent and identically distributed (i.i.d.). Let z denote the normalized outputs of input feature x through $f_h := (h \circ f)(\cdot)$. Consequently, $z^+ = f_h(x^+)$ is the positive embedding of $z = f_h(x)$, and $z_i{}^- = f_h(x_i^-)$ represents the embedding of the samples in the negative pool $\mathcal{N}_x$.

The most common form of the CL loss ($\mathcal{L}_{\text{CL}}$) adapts the earlier InfoNCE loss (Oord et al., 2018) and is formulated as:

$$\mathcal{L}_{\text{CL}} = \underset{\substack{p(x,x^+) \\ \left\{p_n(x_i^-)\right\}_{i=1}^{|\mathcal{N}_x|}}}{\mathbb{E}} \left[-\log \frac{\exp\left(z \cdot z^+ / \tau\right)}{\sum\limits_{i \in [|\mathcal{N}_x|]} \exp\left(z \cdot z_i^- / \tau\right)} \right] \tag{1}$$

where $\tau > 0$ is the temperature parameter. The minimization of the CL loss contributes to learning an embedding space where samples from the positive pair are pulled closer and samples of the negative pair are pushed apart. However, the CL loss is typically used in the **unsupervised pre-training** (Chen et al., 2020; He et al., 2020; Grill et al., 2020) setting. To adapt it to **domain generalization** (Yao et al., 2022; Chen et al., 2022; Kim et al., 2021), the full model is also required to learn from supervised signals. Thus, it is intuitive to combine the CL loss with the empirical risk minimization (ERM) loss $\mathcal{L}_{\text{ERM}}$ as the following objective:

$$\mathcal{L} = \mathcal{L}_{\text{ERM}} + \lambda \mathcal{L}_{\text{CL}} \tag{2}$$

where λ is the regularization parameter. In practice, $\mathcal{L}_{\text{ERM}}$ is usually chosen as the softmax cross entropy loss to classify the output embedding z; we follow the classical setting (as well as the previous studies) in this paper. We note that contrastive learning is only performed during training to regularize the learned representations.

3 Proposed Methodology

We will shortly revisit the recent theoretical understanding of CL (Wang et al., 2022b), and show how the implications from CL theory motivate the design of DCCL for domain generalization.

3.1 Implications from contrastive learning theory

We take a recent study on contrastive learning (Wang et al., 2022b) as the main tool to analyze the failure of self-contrastive learning in the previous subsection. Their analysis shows the ERM loss (the pure classification loss) is mainly impacted by the intra-class conditional variance of the learned representation, and the usage of CL can help reduce the intra-class conditional variance, thus controlling the ERM loss.

The magic comes from the intra-class data connectivity enforced by CL. In applying CL, proper data augmentation can help "connect" two different samples x_i, x_j within the same class, which technically means there exists a pair of augmentation maps a_i, a_j so that $a_i(x_i), a_j(x_j)$ are close to each other. As pushed in optimizing the CL loss (1), the ultimate representations $f_h(x_i), f_h(x_j)$ will finally be close since

$$f_h(x_i) \approx f_h\left(a_i(x_i)\right) \approx f_h\left(a_j(x_j)\right) \approx f_h(x_j).$$

In other words, as a ladder, $a_i(x_i), a_j(x_j)$ connect the two samples x_i, x_j, and analogously all the samples within the same class will be connected by proper data augmentation. CL later on pushes their new representations to cluster thanks to the CL loss.

To illustrate the statement above, we construct a toy classification task in Appendix C, where data augmentation is removed. SCL in this example fails to obtain intra-class connectivity due to insufficient data augmentation and domain-separated (rather than class-separated) representations, which ultimately causes poor classification performance. We further remark a similar idea of leveraging the sample similarities in the same class has been studied by Arjovsky et al. (2019, invariant risk minimization), while the CL theory removes the limitation that the marginal distribution on source domains should be the same on target domains, and thus is theoretically more applicable to DG.

3.2 More aggressive data augmentation and cross-domain positive samples

Inspired by the theoretical analysis above, in this subsection we propose two direct approaches to improve intra-class connectivity: (i) applying more aggressive data augmentation and (ii) expanding the scope of positive samples, from solely self-augmented outputs $a(x)$ to the augmentation of intra-class samples across domains.

For the first approach, in spite of the fact that data augmentation in DG (such as horizontal flipping and color jittering) has already been a standard regularization technique (Gulrajani & Lopez-Paz, 2020; Cha et al., 2021; Wang et al., 2022a), the choice of data augmentation, we emphasize, matters for contrastive learning in the domain generalization setting. We naturally need a larger augmentation distribution $\mathcal{A}$ to connect $a_i(x_i)$ and $a_j(x_j)$ since x_i, x_j can be drawn from different domains. As ablation studies, the effect of data augmentation intensity is evaluated in Section 4.3.

Motivated by supervised CL (Khosla et al., 2020; Gunel et al., 2020; Cui et al., 2021), we further introduce **cross-domain** positive pairs into contrastive learning to bridge the intra-class samples scattered in different domains. Specifically, we not only consider the correlated views of the same data sample as positive pairs but also the augmented instances from other intra-class samples across domains. The positive sample x^+ will now be conditionally independent of x, and the positive pairs have the same conditional distribution $p^{(1)}(x^+|y) = p(x|y)$ [2] (the specific distribution of the positive sample x^+ in this subsection will be denoted with a superscript (1)); in other words, x^+ can now be the augmentation view of a random sample within the same class y of x. With the joint distribution of x, x^+ denoted as $p^{(1)}\left(x, x^+\right) = \int_y p^{(1)}(x^+|y)p(x|y)p(y)\mathrm{d}y$, the primal domain-

[2] Unlike the classical setting in self-supervised CL, in DG we can access the label y in training.

connecting contrastive learning (DCCL) objective $\mathcal{L}^{(0)}_{\texttt{DCCL}}$ can be formulated as:

$$\mathcal{L}^{(0)}_{\texttt{DCCL}} = \mathop{\mathbb{E}}_{\substack{p^{(1)}(x,x^+)\\ \left\{p_n\left(x_i^-\right)\right\}_{i=1}^{|\mathcal{N}_x|}}} \left[-\log \frac{\exp\left(z\cdot z^+/\tau\right)}{\sum\limits_{i\in[|\mathcal{N}_x|]} \exp\left(z\cdot z_i^-/\tau\right)} \right]. \tag{3}$$

Without the explicit use of domain information, $-\log\exp\left(z\cdot z^+/\tau\right)$, the term corresponding to alignment in loss (3), can now push the intra-class samples from different domains together.

3.3 Anchoring learned maps to pre-trained models

Up to now, we have not addressed the core difficulty in domain generalization—lack of access to the testing domains in training: CL is originally designed for the self-supervised scenario where a huge amount and wide range of data are fed to the models. However, in the context of domain generalization, the model is just fine-tuned on limited data within partial domains. Consequently, the mechanism of CL can only contribute to the clustering of representations in the seen domains, while the embeddings of the unseen testing domains and the ones of the training domains in the same class may still be separated.

Interestingly, the intra-class connectivity for representations, the desired property in CL, seems to exist at the beginning of the fine-tuning. We observe the phenomenon when visualizing the representations obtained from the pre-trained model using t-SNE (Van der Maaten & Hinton, 2008) in Figure 4a, which thereby motivates our design in this subsection. We can find that mapped by the initial pre-trained model ResNet-50, intra-class samples of the training domains and the testing domains are scattered while well-connected.

We attribute the phenomenon to the effective representations returned by pre-trained model, which reasonably model the pairwise interactions among images and thus draw target domains closer to source domains. To verify the effectiveness of the representations, we design a quantitative **metric to evaluate** whether the pre-trained space is "well-connected", by turning to the concept of "connectivity" in graphs. Details can be found in Appendix A.4.

As for the model design, the phenomenon motivates us to better utilize the pre-trained model f_{pre} for stronger intra-class connectivity in the mapped representations obtained from f. We propose to take the usage of pre-trained models as data augmentation in a disguised form: regular data augmentation works on the raw data and return x while we can further "augment" the representation x via f_{pre}.

In mathematical language, we descibe our design as follows. Upon the augmented sample x defined in the last subsection, we further incorporate the pre-trained embedding $z_{\text{pre}} = h\circ f_{\text{pre}}(x)$ into the definition of feasible positive embeddings $z^{(2),+}$, which expands the scope of the previous positive embeddings z^+ (the superscript (2) implies the different distribution compared to z^+ in the last subsection). In particular, for a given x, we decide the form of the newly coined positive embedding $z^{(2),+}$ as:

$$z^{(2),+} = \begin{cases} z^+ = h\circ f(x^+), & \text{w.p. } \frac{1}{2}, \\ z_{\text{pre}} = h\circ f_{\text{pre}}(x), & \text{w.p. } \frac{1}{2}. \end{cases}$$

With the distribution of the extended positive embedding denoted as $p^{(2)}\left(z^{(2),+}\right)$ (the positive pairs x, x^+ still follow $p^{(1)}(x,x^+)$), the proposed DCCL loss $\mathcal{L}_{\texttt{DCCL}}$ can be written as:

$$\mathcal{L}_{\texttt{DCCL}} = \mathop{\mathbb{E}}_{\substack{p^{(2)}\left(z,z^{(2),+}\right)\\ \left\{p_n\left(x_i^-\right)\right\}_{i=1}^{|\mathcal{N}_x|}}} \left[-\log \frac{\exp\left(z\cdot z^{(2),+}/\tau\right)}{\sum\limits_{i\in[|\mathcal{N}_x|]} \exp\left(z\cdot z_i^-/\tau\right)} \right], \tag{4}$$

where $p^{(2)}\left(z, z^{(2),+}\right)$ is the joint distribution of $z, z^{(2),+}$ constructed in this subsection.

3.4 Generative transformation loss for pre-trained representation

In the previous section, our proposed contrastive learning method manages to mine the supervised signal at the **inter-sample** level, where we align the positive pairs (composed of different samples) while pushing apart the samples in a negative pool.

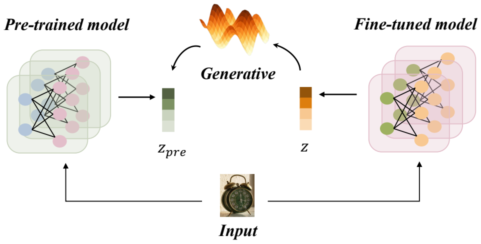

Figure 3: An overview of the generative transformation module in DCCL. Two representations z_{pre} and z of the same image are generated via the pre-trained and the fine-tuned model respectively. The variational reconstruction is conducted to encode essential within-sample information.

Echoing the findings in (Yao et al., 2022), which point out that directly aligning positive pairs across vastly different domains often results in poor performance, our research similarly identifies a substantial gap in the representations of pre-trained and fine-tuned models. Direct alignment using contrastive learning as evidenced by our empirical evaluation, tends to be sub-optimal. In response, we introduce the concept of variational generative loss to comprehend the transformation process and bridge these representational gaps. Additionally, the generative transformation module is designed to reconstruct the features of the pre-trained model at an intra-sample level. This complements the inter-sample level supervision provided by contrastive loss. The module, along with its associated loss function, is intended to provide a more enriched supervised signal, encapsulating crucial within-sample information. This module, in turn, supports as a pivotal proxy objective that facilitates model anchoring 3.3.

To simplify the notation of the transformation, we abuse the previous notations $\{z, z_{\text{pre}}\}$ for the output embedding from a certain learned/pre-trained model layer, omitting the corresponding layer denotation. z_{pre} is the fixed supervised signal provided by the pre-trained model.

With the notation $\{z, z_{\text{pre}}\}$, we introduce the following variational generative model to parameterize the map $g : z \mapsto z_{\text{pre}}$ relating the representation manifolds formed by (the first several layers of) the learned map f and the fixed pre-trained model f_{pre}. In particular, g is composed of an encoder ϕ modeling a tunable conditional distribution $q_\phi\left(z_{\text{lat}} \mid z\right)$ of z_{lat} and a tunable decoder ψ mapping z_{lat} back to z_{pre}, in which $z_{\text{lat}} \in \mathbb{R}^{d'}$ is the latent representation of the generator. Similar to the training of a regular variational autoencoder (VAE) (Kingma et al., 2019), the latent variable z_{lat} will be sampled from $q_\phi\left(z_{\text{lat}} \mid z\right)$; we can then project z_{lat} to the pre-trained embedding space via decoder ψ. Our variational reconstruction loss $\mathcal{L}_{\text{DCCL}}^{\text{Gen}}$ is designed as:

$$\mathcal{L}_{\text{DCCL}}^{\text{Gen}} = -\mathbb{E}_{q_\phi\left(z_{\text{lat}} \mid z\right)}\left[\log p_\psi\left(z_{\text{pre}} \mid z_{\text{lat}}\right)\right] + \text{KL}\left[q_\phi\left(z_{\text{lat}} \mid z\right) \| \, p\left(z_{\text{lat}}\right)\right], \tag{5}$$

where $p\left(z_{\text{lat}}\right)$ is the pre-specified prior distribution of z_{lat}, $p_\psi\left(z_{\text{pre}} \mid z_{\text{lat}}\right)$ is decided by the “reconstruction loss” $\|z_{\text{pre}} - \psi\left(z_{\text{lat}}\right)\|^2$, and the KL divergence term corresponds to the variational regularization term to avoid mode collapse. The workflow of our proposed generative transformation is shown in Figure 3.

Finally, to benefit the representation learning through both generative transformation and our improved contrastive leaning, we set our ultimate objective as:

$$\mathcal{L} = \mathcal{L}_{\text{ERM}} + \lambda \mathcal{L}_{\text{DCCL}} + \beta \mathcal{L}_{\text{DCCL}}^{\text{Gen}} \tag{6}$$

where λ and β are coefficients to balance the multi-task loss. The ablation studies in Section 4.3 verify the effectiveness of each component.

4 EXPERIMENTS

In this section, we empirically evaluate the performance of our proposed DCCL, intending to answer the following research questions:

- **RQ1:** Does DCCL enable networks to learn transferable representation under distribution shifts?
- **RQ2:** How do different components in our framework contribute to the performance?
- **RQ3:** How good is the generalizability of our proposed DCCL under different circumstances (e.g., varying label ratios and backbones)?
- **RQ4:** Does DCCL really connect the cross-domain representations?

4.1 EXPERIMENTAL SETTINGS

We exhaustively evaluate out-of-domain (OOD) accuracy of DCCL on various representative DG benchmarks as in Cha et al. (2021); Yao et al. (2022); Cha et al. (2022); Chen et al. (2022): Office-

Algorithm	A	C	P	S	Avg.
IRM (Arjovsky et al., 2019)	84.8	76.4	96.7	76.1	83.5
MetaReg (Balaji et al., 2018)	87.2	79.2	97.6	70.3	83.6
DANN (Ganin et al., 2016)	86.4	77.4	97.3	73.5	83.7
ERM (Vapnik, 1999)	85.7	77.1	97.4	76.6	84.2
GroupDRO (Ganin et al., 2016)	83.5	79.1	96.7	78.3	84.4
MTL (Blanchard et al., 2021)	87.5	77.1	96.4	77.3	84.6
I-Mixup (Xu et al., 2020)	86.1	78.9	97.6	75.8	84.6
MMD (Li et al., 2018b)	86.1	79.4	96.6	76.5	84.7
VREx (Krueger et al., 2021)	86.0	79.1	96.9	77.7	84.9
MLDG (Li et al., 2018a)	85.5	80.1	97.4	76.6	84.9
ARM (Zhang et al., 2020)	86.8	76.8	97.4	79.3	85.1
RSC (Huang et al., 2020)	85.4	79.7	97.6	78.2	85.2
Mixstyle (Zhou et al., 2021)	86.8	79.0	96.6	78.5	85.2
ER (Zhao et al., 2020)	87.5	79.3	**98.3**	76.3	85.3
pAdaIN (Nuriel et al., 2021)	85.8	81.1	97.2	77.4	85.4
SelfReg (Kim et al., 2021)	85.0	81.0	95.9	80.5	85.6
EISNet (Wang et al., 2020)	86.6	81.5	97.1	78.1	85.8
CORAL (Sun & Saenko, 2016)	88.3	80.0	97.5	78.8	86.2
SagNet (Nam et al., 2021)	87.4	80.7	97.1	80.0	86.3
DSON (Seo et al., 2020)	87.0	80.6	96.0	82.9	86.6
COMEN (Chen et al., 2022)	88.1	82.6	97.2	81.9	87.5
SWAD (Cha et al., 2021)	89.3	83.4	97.3	82.5	88.1
MIRO (Cha et al., 2022)	89.8	83.6	98.2	82.1	88.4
PCL (Yao et al., 2022)	90.2	83.9	98.1	82.6	88.7
Ours	**90.5**	**84.2**	98.0	**83.3**	**89.1± 0.1**

(a) PACS

Algorithm	A	C	P	R	Avg
Mixstyle (Zhou et al., 2021)	51.1	53.2	68.2	69.2	60.4
IRM (Arjovsky et al., 2019)	58.9	52.2	72.1	74.0	64.3
ARM (Zhang et al., 2020)	58.9	51.0	74.1	75.2	64.8
RSC (Huang et al., 2020)	60.7	51.4	74.8	75.1	65.5
CDANN (Li et al., 2018b)	61.5	50.4	74.4	76.6	65.7
DANN (Ganin et al., 2016)	59.9	53.0	73.6	76.9	65.9
GroupDRO (Ganin et al., 2016)	60.4	52.7	75.0	76.0	66.0
MMD (Li et al., 2018b)	60.4	53.3	74.3	77.4	66.4
MTL (Blanchard et al., 2021)	61.5	52.4	74.9	76.8	66.4
VREx (Krueger et al., 2021)	60.7	53.0	75.3	76.6	66.4
MLDG (Li et al., 2018a)	61.5	53.2	75.0	77.5	66.8
ERM (Vapnik, 1999)	63.1	51.9	77.2	78.1	67.6
SelfReg (Kim et al., 2021)	63.6	53.1	76.9	78.1	67.9
I-Mixup (Xu et al., 2020)	62.4	54.8	76.9	78.3	68.1
SagNet (Nam et al., 2021)	63.4	54.8	75.8	78.3	68.1
CORAL (Sun & Saenko, 2016)	65.3	54.4	76.5	78.4	68.7
COMEN (Chen et al., 2022)	65.4	55.6	75.8	78.9	68.9
SWAD (Cha et al., 2021)	66.1	57.7	78.4	80.2	70.6
PCL (Yao et al., 2022)	67.3	**59.9**	78.7	80.7	71.6
MIRO (Cha et al., 2022)	68.8	58.1	79.9	82.6	72.4
Ours	**70.1**	59.1	**81.4**	**83.4**	$\mathbf{73.5 \pm 0.2}$

(b) Office-Home

Table 1: Experimental comparisons with state-of-the-art methods on benchmarks with ResNet-50. (The tables are re-scaled due to space limit.)

Home (Venkateswara et al., 2017), PACS (Li et al., 2017), VLCS (Fang et al., 2013), TerraIncognita (Beery et al., 2018), and DomainNet (Peng et al., 2019). The details of the data sets are shown in Appendix A.1. For fair comparison, we strictly follow the experimental settings in Gulrajani & Lopez-Paz (2020); Cha et al. (2021); Yao et al. (2022); Chen et al. (2022) and adopt the widely used leave-one-domain-out evaluation protocol, i.e., one domain is chosen as the held-out testing domain and the rest are regarded as source training domains. The experiment results are all averaged over three repeated runs. Following DomainBed (Gulrajani & Lopez-Paz, 2020), we leave 20% of source domain data for validation and model selection. As in previous works (Cha et al., 2022; Yao et al., 2022), we use the ResNet-50 model pre-trained on ImageNet by default, and our code is mainly built upon DomainBed (Gulrajani & Lopez-Paz, 2020) and SWAD (Cha et al., 2021). Due to space constraints, detailed implementation and experimental setups are shown in Appendix A.1. The limitations, attribution of existing assets, and the use of personal data are discussed in Appendix D.

4.2 RESULTS (RQ1)

We provide comprehensive comparisons with a set of strong baselines on the domain generalization benchmarks, PACS and OfficeHome, in Tables 1a and 1b. Detailed experimental results on TerraIncognita, VLCS, and DomainNet datasets are deferred to Appendix A.2. We observe our proposed method achieves the best performance: the metrics are 44.0 (ERM)$\rightarrow$47.0 (Best Baseline)$\rightarrow$47.5 (Ours) on DomainNet, 77.3$\rightarrow$79.6$\rightarrow$80.0 on VLCS, and 47.8$\rightarrow$52.9$\rightarrow$53.7 on TerraIncognita. The results of the intermediate columns in the tables represent performance on the testing domain. For example, "A" in Table 1 denotes testing on domain Art and training on Photo, Cartoon, and Sketch. The final result is averaged over all domains. The symbol + in the tables is used to denote that the reproduced experimental performance is clearly distinct from the reported one (such as "PCL$^+$" in Table 4). All the baselines are sorted in ascending order of their performance.

We have the following findings from the tables. (i) We find that `DCCL` substantially outperforms all the baseline methods concerning OOD accuracy. This indicates the capability of `DCCL` to extract transferable representation for generalization under distribution shift. (ii) We notice most baselines make explicit use of domain supervision, while only a few methods such as RSC (Huang et al., 2020), SagNet (Nam et al., 2021), COMEN (Chen et al., 2022), SWAD (Cha et al., 2021), MIRO (Cha et al., 2022) and our `DCCL` do not. The excellent performance of our `DCCL` may reveal previous works do not well utilize the domain information and there is still much room for improvement. (iii) We note that PCL (Yao et al., 2022) (Proxy Contrastive Learning) has utilized the potential of CL, aligns embeddings of different samples into domain centers, and consistently achieves good performance. Meanwhile, MIRO (Cha et al., 2022) also preserves the pre-trained features by adding the mutual information regularization term and attains satisfactory performance. However, because

CDC	PMA	GT	A	C	P	R	Avg.
-	-	-	66.1	57.7	78.4	80.2	70.6
with Self-Contrast			65.4	51.4	79.1	79.5	68.9
✓	-	-	68.0	57.9	80.1	81.3	71.8
-	✓	-	68.8	57.8	80.4	82.3	72.3
-	-	✓	69.0	56.9	80.6	81.6	72.0
-	✓	✓	70.0	58.7	80.5	83.4	73.1
✓	✓	-	69.2	58.5	81.0	83.0	72.9
✓	-	✓	69.0	58.5	80.7	82.1	72.6
w/o Aggressive Aug			69.8	58.6	81.0	82.6	73.0
✓	✓	✓	**70.1**	**59.1**	**81.4**	**83.4**	**73.5**

Table 2: Ablation Studies of DCCL on OfficeHome.

Ratio	Algorithm	A	C	P	R	Avg.
5%	ERM (Vapnik, 1999)	40.4	32.6	42.6	49.2	41.2
	SWAD (Cha et al., 2021)	46.9	36.2	48.5	54.2	46.4
	COMEN (Chen et al., 2022)	47.7	39.2	50.6	56.1	48.4
	PCL (Yao et al., 2022)	48.4	42.3	55.2	57.2	50.8
	MIRO (Cha et al., 2022)	51.0	41.6	58.6	61.5	53.2
	Ours	**55.7**	**44.1**	**63.1**	**67.1**	**57.5 (+16.3)**
10%	ERM (Vapnik, 1999)	45.1	41.9	55.9	58.0	50.2
	COMEN (Chen et al., 2022)	50.4	44.3	56.8	60.9	53.1
	SWAD (Cha et al., 2021)	53.3	43.9	61.8	65.2	56.1
	PCL (Yao et al., 2022)	54.6	45.1	60.9	67.2	57.0
	MIRO (Cha et al., 2022)	58.9	46.6	68.6	71.7	61.4
	Ours	**62.5**	**49.2**	**72.3**	**75.1**	**64.8 (+14.6)**

Table 3: Experimental comparisons of DCCL with representative baselines on OfficeHome under various label ratios.

of their deficiency to connect cross-domain representations, our method manages to improve upon the success the previous baselines had.

4.3 Ablation studies (RQ2)

In this part, we investigate the effectiveness of the proposed DCCL by evaluating the impact of different components. We denote the Cross-Domain Contrastive learning in Section 3.2 as CDC (with more aggressive data augmentation and cross-domain positive samples), Pre-trained Model Anchoring in Section 3.3 as PMA, and Generative Transformation in Section 3.4 as GT. The ablation results are summarized in Table 2. The check mark in the table indicates the module is incorporated. We note that our improved contrastive learning loss in Eqn. (4) has two components: CDC and PMA. The overall improvement of the loss is substantial: $70.6 \rightarrow 72.9$. From the table, we can observe that all the components are useful: when any one of these components is removed, the performance drops accordingly. For example, removing PMA module leads to significant performance degeneration, which verifies the importance of anchoring learned maps to pre-trained models. We can then find the combination of PMA and GT leads to the highest improvement in the ablation, which indicates GT and PMA modules complement each other in an effective way. The finding is also consistent with our motivation in Section 3.4. Moreover, we also evaluate self-contrastive learning. The experimental results indicate that self-contrastive learning will distort the learned embeddings and hamper performance. Besides, the experiment without aggressive data augmentation also validates the effectiveness of stronger data augmentations we suggest in Section 3.2. Additional experimental details and explanations regarding our choices for VAE structures, contrastive learning techniques within DCCL, cross-domain examples in CDC, alternative pre-trained backbones, and the Wilds Benchmark can be found in Appendix A.5.

4.4 Case studies

Generalization ability (RQ3). To verify the generalizability of our proposed DCCL, we conduct experiments[3] with different label ratios (the percentage of labeled training data) and backbones. (i) In Table 3, we find DCCL can obtain consistent improvement over baselines, in both cases of 5% and 10% label ratios. Our method yields a 16.3 and 14.6 absolute improvement compared with

[3] We select a few of the most representative methods as baselines.

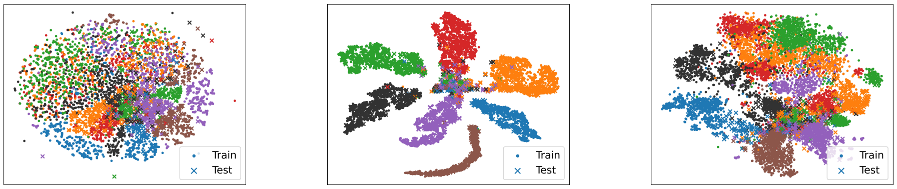

(a) Pre-trained. (b) ERM. (c) SCL.

Figure 4: t-SNE visualization of the representations across both training and testing domains, output by Pre-trained, ERM, and SCL respectively. Same-class points are in the same colors, and two marker types differentiate the training or the testing domains. We visualize the embedding on PACS dataset where the source domains are Photo, Sketch, and Cartoon; the target domain is Art.

Algorithm	A	C	P	R	Avg.
ERM (Vapnik, 1999)	50.6	49.0	69.9	71.4	60.2
SWAD (Cha et al., 2021)	54.6	50.0	71.1	72.8	62.1
PCL$^+$ (Yao et al., 2022)	58.8	51.9	74.2	75.2	65.0
MIRO (Cha et al., 2022)	59.7	52.6	75.0	77.7	66.2
COMEN (Chen et al., 2022)	57.6	**55.8**	75.5	76.9	66.5
“Mismatch”	53.4	50.7	72.3	74.0	62.6
Ours	**61.7**	53.6	**75.9**	**78.7**	**67.5**

Table 4: Experimental comparisons of DCCL on OfficeHome with the ResNet-18 backbone in use.

ERM. We can observe that as the number of available labels reduces, the model benefits more from our DCCL (compared with previous 67.6→73.5 increase under 100% label ratio in Table 1b). (ii) In Table 4, we test the performance with a new backbone, ResNet-18 (previously ResNet-50)[4]. We find that even though the baselines' relative ordering changes significantly, our model still performs the best, showcasing the robustness thereof. We further observe replacing the ResNet-18 pre-trained representations to the larger ResNet-50 ones (“mismatch” between the backbone used for fine-tuning and the pre-trained representations) will cause substantial performance drop 67.5 → 62.6.

Analysis of the representations in DCCL (RQ4). We analyze the representations returned by DCCL to provide more insights. In Figure 4, we utilize t-SNE (Van der Maaten & Hinton, 2008) to visualize the embeddings of the pre-trained model, ERM, and SCL model. We can observe that mapped by the original pre-trained model ResNet-50, the intra-class samples of the training domains and the testing domains are scattered while well-connected. However, in the ERM model, many samples in the testing domain are distributed in the central part of the plot, which is separated from the training samples. There is a clear gap between the training and the testing domains. As for SCL, it seems to harm the learned embedding space and distort the class decision boundary. The observations verify our conjectures in Section C.

We then visualize the embeddings of ERM, PCL, and our DCCL methods on the testing domains in Appendix A.3. Our DCCL learns discriminative representations even in the unseen target domain by enhancing intra-class connectivity in CL, which is not addressed in ERM and PCL.

5 Conclusions

In this paper, we revisit the role of contrastive learning in domain generalization and identify a key factor: intra-class connectivity. We analyze the failure of directly applying contrastive learning to DG and propose two strategies to improve intra-class connectivity: (i) applying more aggressive data augmentation and (ii) expanding the scope of positive samples. Moreover, to alleviate lack of access to the testing domains in training, we propose to anchor learned maps to pre-trained models which possess the desired connectivity of training and testing domains. Generative transformation is further introduced to complement the pre-trained alignment. Consequently, we combine the pieces together and propose DCCL to enable robust representations in the out-of-domain scenario. Extensive experiments on 5 real-world datasets demonstrate the effectiveness of DCCL, which outperforms a bundle of baselines.

[4] For semantic information matching, pre-trained representations in DCCL are generated from the same backbone model used for fine-tuning.

References

Martin Arjovsky, Léon Bottou, Ishaan Gulrajani, and David Lopez-Paz. Invariant risk minimization. *arXiv preprint arXiv:1907.02893*, 2019.

Yogesh Balaji, Swami Sankaranarayanan, and Rama Chellappa. Metareg: Towards domain generalization using meta-regularization. In *Advances in Neural Information Processing Systems 31: Annual Conference on Neural Information Processing Systems 2018, NeurIPS 2018, December 3-8, 2018, Montréal, Canada*, pp. 1006–1016, 2018.

Sara Beery, Grant Van Horn, and Pietro Perona. Recognition in terra incognita. In *Proceedings of the European conference on computer vision (ECCV)*, pp. 456–473, 2018.

Gilles Blanchard, Aniket Anand Deshmukh, Ürun Dogan, Gyemin Lee, and Clayton Scott. Domain generalization by marginal transfer learning. *The Journal of Machine Learning Research*, 22(1): 46–100, 2021.

Mathilde Caron, Ishan Misra, Julien Mairal, Priya Goyal, Piotr Bojanowski, and Armand Joulin. Unsupervised learning of visual features by contrasting cluster assignments. *Advances in neural information processing systems*, 33:9912–9924, 2020.

Junbum Cha, Sanghyuk Chun, Kyungjae Lee, Han-Cheol Cho, Seunghyun Park, Yunsung Lee, and Sungrae Park. Swad: Domain generalization by seeking flat minima. *Advances in Neural Information Processing Systems*, 34:22405–22418, 2021.

Junbum Cha, Kyungjae Lee, Sungrae Park, and Sanghyuk Chun. Domain generalization by mutual-information regularization with pre-trained models. In *ECCV*, 2022.

Prithvijit Chattopadhyay, Yogesh Balaji, and Judy Hoffman. Learning to balance specificity and invariance for in and out of domain generalization. In *European Conference on Computer Vision*, pp. 301–318. Springer, 2020.

Chaoqi Chen, Jiongcheng Li, Xiaoguang Han, Xiaoqing Liu, and Yizhou Yu. Compound domain generalization via meta-knowledge encoding. In *Proceedings of the IEEE/CVF Conference on Computer Vision and Pattern Recognition*, pp. 7119–7129, 2022.

Ting Chen, Simon Kornblith, Mohammad Norouzi, and Geoffrey E. Hinton. A simple framework for contrastive learning of visual representations. In *Proceedings of the 37th International Conference on Machine Learning, ICML 2020, 13-18 July 2020, Virtual Event*, volume 119 of *Proceedings of Machine Learning Research*, pp. 1597–1607. PMLR, 2020.

Xinlei Chen and Kaiming He. Exploring simple siamese representation learning. In *Proceedings of the IEEE/CVF Conference on Computer Vision and Pattern Recognition*, pp. 15750–15758, 2021.

Bowen Cheng, Alex Schwing, and Alexander Kirillov. Per-pixel classification is not all you need for semantic segmentation. *Advances in Neural Information Processing Systems*, 34:17864–17875, 2021.

Xu Chu, Yujie Jin, Wenwu Zhu, Yasha Wang, Xin Wang, Shanghang Zhang, and Hong Mei. Dna: Domain generalization with diversified neural averaging. In *International Conference on Machine Learning*, pp. 4010–4034. PMLR, 2022.

Jiequan Cui, Zhisheng Zhong, Shu Liu, Bei Yu, and Jiaya Jia. Parametric contrastive learning. In *Proceedings of the IEEE/CVF international conference on computer vision*, pp. 715–724, 2021.

Babak Esmaeili, Hao Wu, Sarthak Jain, Alican Bozkurt, Narayanaswamy Siddharth, Brooks Paige, Dana H Brooks, Jennifer Dy, and Jan-Willem Meent. Structured disentangled representations. In *The 22nd International Conference on Artificial Intelligence and Statistics*, pp. 2525–2534. PMLR, 2019.

Chen Fang, Ye Xu, and Daniel N. Rockmore. Unbiased metric learning: On the utilization of multiple datasets and web images for softening bias. In *IEEE International Conference on Computer Vision, ICCV 2013, Sydney, Australia, December 1-8, 2013*, pp. 1657–1664. IEEE Computer Society, 2013.

Chelsea Finn, Pieter Abbeel, and Sergey Levine. Model-agnostic meta-learning for fast adaptation of deep networks. In *Proceedings of the 34th International Conference on Machine Learning, ICML 2017, Sydney, NSW, Australia, 6-11 August 2017*, volume 70 of *Proceedings of Machine Learning Research*, pp. 1126–1135. PMLR, 2017.

Yaroslav Ganin, Evgeniya Ustinova, Hana Ajakan, Pascal Germain, Hugo Larochelle, François Laviolette, Mario Marchand, and Victor Lempitsky. Domain-adversarial training of neural networks. *The journal of machine learning research*, 17(1):2096–2030, 2016.

Tianyu Gao, Xingcheng Yao, and Danqi Chen. Simcse: Simple contrastive learning of sentence embeddings. *arXiv preprint arXiv:2104.08821*, 2021.

Jean-Bastien Grill, Florian Strub, Florent Altché, Corentin Tallec, Pierre H. Richemond, Elena Buchatskaya, Carl Doersch, Bernardo Ávila Pires, Zhaohan Guo, Mohammad Gheshlaghi Azar, Bilal Piot, Koray Kavukcuoglu, Rémi Munos, and Michal Valko. Bootstrap your own latent - A new approach to self-supervised learning. In *Advances in Neural Information Processing Systems 33: Annual Conference on Neural Information Processing Systems 2020, NeurIPS 2020, December 6-12, 2020, virtual*, 2020.

Ishaan Gulrajani and David Lopez-Paz. In search of lost domain generalization. *arXiv preprint arXiv:2007.01434*, 2020.

Beliz Gunel, Jingfei Du, Alexis Conneau, and Ves Stoyanov. Supervised contrastive learning for pre-trained language model fine-tuning. *arXiv preprint arXiv:2011.01403*, 2020.

Kaiming He, Xiangyu Zhang, Shaoqing Ren, and Jian Sun. Deep residual learning for image recognition. In *2016 IEEE Conference on Computer Vision and Pattern Recognition, CVPR 2016, Las Vegas, NV, USA, June 27-30, 2016*, pp. 770–778. IEEE Computer Society, 2016.

Kaiming He, Haoqi Fan, Yuxin Wu, Saining Xie, and Ross B. Girshick. Momentum contrast for unsupervised visual representation learning. In *2020 IEEE/CVF Conference on Computer Vision and Pattern Recognition, CVPR 2020, Seattle, WA, USA, June 13-19, 2020*, pp. 9726–9735. IEEE, 2020.

R. Devon Hjelm, Alex Fedorov, Samuel Lavoie-Marchildon, Karan Grewal, Philip Bachman, Adam Trischler, and Yoshua Bengio. Learning deep representations by mutual information estimation and maximization. In *7th International Conference on Learning Representations, ICLR 2019, New Orleans, LA, USA, May 6-9, 2019*. OpenReview.net, 2019.

Huaibo Huang, Ran He, Zhenan Sun, Tieniu Tan, et al. Introvae: Introspective variational autoencoders for photographic image synthesis. *Advances in neural information processing systems*, 31, 2018.

Zeyi Huang, Haohan Wang, Eric P Xing, and Dong Huang. Self-challenging improves cross-domain generalization. In *European Conference on Computer Vision*, pp. 124–140. Springer, 2020.

Prannay Khosla, Piotr Teterwak, Chen Wang, Aaron Sarna, Yonglong Tian, Phillip Isola, Aaron Maschinot, Ce Liu, and Dilip Krishnan. Supervised contrastive learning. In *Advances in Neural Information Processing Systems 33: Annual Conference on Neural Information Processing Systems 2020, NeurIPS 2020, December 6-12, 2020, virtual*, 2020.

Daehee Kim, Youngjun Yoo, Seunghyun Park, Jinkyu Kim, and Jaekoo Lee. Selfreg: Self-supervised contrastive regularization for domain generalization. In *Proceedings of the IEEE/CVF International Conference on Computer Vision*, pp. 9619–9628, 2021.

Diederik P. Kingma and Jimmy Ba. Adam: A method for stochastic optimization. In *3rd International Conference on Learning Representations, ICLR 2015, San Diego, CA, USA, May 7-9, 2015, Conference Track Proceedings*, 2015.

Diederik P Kingma, Max Welling, et al. An introduction to variational autoencoders. *Foundations and Trends® in Machine Learning*, 12(4):307–392, 2019.

David Krueger, Ethan Caballero, Joern-Henrik Jacobsen, Amy Zhang, Jonathan Binas, Dinghuai Zhang, Remi Le Priol, and Aaron Courville. Out-of-distribution generalization via risk extrapolation (rex). In *International Conference on Machine Learning*, pp. 5815–5826. PMLR, 2021.

Da Li, Yongxin Yang, Yi-Zhe Song, and Timothy M. Hospedales. Deeper, broader and artier domain generalization. In *IEEE International Conference on Computer Vision, ICCV 2017, Venice, Italy, October 22-29, 2017*, pp. 5543–5551. IEEE Computer Society, 2017.

Da Li, Yongxin Yang, Yi-Zhe Song, and Timothy M. Hospedales. Learning to generalize: Meta-learning for domain generalization. In *Proceedings of the Thirty-Second AAAI Conference on Artificial Intelligence, (AAAI-18), the 30th innovative Applications of Artificial Intelligence (IAAI-18), and the 8th AAAI Symposium on Educational Advances in Artificial Intelligence (EAAI-18), New Orleans, Louisiana, USA, February 2-7, 2018*, pp. 3490–3497. AAAI Press, 2018a.

Haoliang Li, Sinno Jialin Pan, Shiqi Wang, and Alex C. Kot. Domain generalization with adversarial feature learning. In *2018 IEEE Conference on Computer Vision and Pattern Recognition, CVPR 2018, Salt Lake City, UT, USA, June 18-22, 2018*, pp. 5400–5409. IEEE Computer Society, 2018b.

Pan Li, Da Li, Wei Li, Shaogang Gong, Yanwei Fu, and Timothy M Hospedales. A simple feature augmentation for domain generalization. In *Proceedings of the IEEE/CVF International Conference on Computer Vision*, pp. 8886–8895, 2021.

Sihang Li, Xiang Wang, An Zhang, Yingxin Wu, Xiangnan He, and Tat-Seng Chua. Let invariant rationale discovery inspire graph contrastive learning. In *International Conference on Machine Learning*, pp. 13052–13065. PMLR, 2022.

Ya Li, Xinmei Tian, Mingming Gong, Yajing Liu, Tongliang Liu, Kun Zhang, and Dacheng Tao. Deep domain generalization via conditional invariant adversarial networks. In *Proceedings of the European Conference on Computer Vision (ECCV)*, pp. 624–639, 2018c.

Yuchen Liu, Yaoming Wang, Yabo Chen, Wenrui Dai, Chenglin Li, Junni Zou, and Hongkai Xiong. Promoting semantic connectivity: Dual nearest neighbors contrastive learning for unsupervised domain generalization. In *Proceedings of the IEEE/CVF Conference on Computer Vision and Pattern Recognition*, pp. 3510–3519, 2023.

Toshihiko Matsuura and Tatsuya Harada. Domain generalization using a mixture of multiple latent domains. In *Proceedings of the AAAI Conference on Artificial Intelligence*, volume 34, pp. 11749–11756, 2020.

Hyeonseob Nam, HyunJae Lee, Jongchan Park, Wonjun Yoon, and Donggeun Yoo. Reducing domain gap by reducing style bias. In *Proceedings of the IEEE/CVF Conference on Computer Vision and Pattern Recognition*, pp. 8690–8699, 2021.

Oren Nuriel, Sagie Benaim, and Lior Wolf. Permuted adain: Reducing the bias towards global statistics in image classification. In *Proceedings of the IEEE/CVF Conference on Computer Vision and Pattern Recognition*, pp. 9482–9491, 2021.

Aaron van den Oord, Yazhe Li, and Oriol Vinyals. Representation learning with contrastive predictive coding. *arXiv preprint arXiv:1807.03748*, 2018.

Xingchao Peng, Qinxun Bai, Xide Xia, Zijun Huang, Kate Saenko, and Bo Wang. Moment matching for multi-source domain adaptation. In *2019 IEEE/CVF International Conference on Computer Vision, ICCV 2019, Seoul, Korea (South), October 27 - November 2, 2019*, pp. 1406–1415. IEEE, 2019.

Fengchun Qiao, Long Zhao, and Xi Peng. Learning to learn single domain generalization. In *2020 IEEE/CVF Conference on Computer Vision and Pattern Recognition, CVPR 2020, Seattle, WA, USA, June 13-19, 2020*, pp. 12553–12562. IEEE, 2020.

Seonguk Seo, Yumin Suh, Dongwan Kim, Geeho Kim, Jongwoo Han, and Bohyung Han. Learning to optimize domain specific normalization for domain generalization. In *European Conference on Computer Vision*, pp. 68–83. Springer, 2020.

Changjian Shui, Boyu Wang, and Christian Gagné. On the benefits of representation regularization in invariance based domain generalization. *Machine Learning*, 111(3):895–915, 2022.

Baochen Sun and Kate Saenko. Deep coral: Correlation alignment for deep domain adaptation. In *European conference on computer vision*, pp. 443–450. Springer, 2016.

Ke Sun, Bin Xiao, Dong Liu, and Jingdong Wang. Deep high-resolution representation learning for human pose estimation. In *IEEE Conference on Computer Vision and Pattern Recognition, CVPR 2019, Long Beach, CA, USA, June 16-20, 2019*, pp. 5693–5703. Computer Vision Foundation / IEEE, 2019.

Mingxing Tan, Ruoming Pang, and Quoc V. Le. Efficientdet: Scalable and efficient object detection. In *2020 IEEE/CVF Conference on Computer Vision and Pattern Recognition, CVPR 2020, Seattle, WA, USA, June 13-19, 2020*, pp. 10778–10787. IEEE, 2020.

Eric Tzeng, Judy Hoffman, Kate Saenko, and Trevor Darrell. Adversarial discriminative domain adaptation. In *2017 IEEE Conference on Computer Vision and Pattern Recognition, CVPR 2017, Honolulu, HI, USA, July 21-26, 2017*, pp. 2962–2971. IEEE Computer Society, 2017.

Laurens Van der Maaten and Geoffrey Hinton. Visualizing data using t-sne. *Journal of machine learning research*, 9(11), 2008.

Vladimir N Vapnik. An overview of statistical learning theory. *IEEE transactions on neural networks*, 10(5):988–999, 1999.

Hemanth Venkateswara, Jose Eusebio, Shayok Chakraborty, and Sethuraman Panchanathan. Deep hashing network for unsupervised domain adaptation. In *2017 IEEE Conference on Computer Vision and Pattern Recognition, CVPR 2017, Honolulu, HI, USA, July 21-26, 2017*, pp. 5385–5394. IEEE Computer Society, 2017.

Riccardo Volpi, Hongseok Namkoong, Ozan Sener, John C. Duchi, Vittorio Murino, and Silvio Savarese. Generalizing to unseen domains via adversarial data augmentation. In *Advances in Neural Information Processing Systems 31: Annual Conference on Neural Information Processing Systems 2018, NeurIPS 2018, December 3-8, 2018, Montréal, Canada*, pp. 5339–5349, 2018.

Jindong Wang, Cuiling Lan, Chang Liu, Yidong Ouyang, Tao Qin, Wang Lu, Yiqiang Chen, Wenjun Zeng, and Philip Yu. Generalizing to unseen domains: A survey on domain generalization. *IEEE Transactions on Knowledge and Data Engineering*, 2022a.

Shujun Wang, Lequan Yu, Caizi Li, Chi-Wing Fu, and Pheng-Ann Heng. Learning from extrinsic and intrinsic supervisions for domain generalization. In *European Conference on Computer Vision*, pp. 159–176. Springer, 2020.

Tongzhou Wang and Phillip Isola. Understanding contrastive representation learning through alignment and uniformity on the hypersphere. In *Proceedings of the 37th International Conference on Machine Learning, ICML 2020, 13-18 July 2020, Virtual Event*, volume 119 of *Proceedings of Machine Learning Research*, pp. 9929–9939. PMLR, 2020.

Yifei Wang, Qi Zhang, Yisen Wang, Jiansheng Yang, and Zhouchen Lin. Chaos is a ladder: A new theoretical understanding of contrastive learning via augmentation overlap. *arXiv preprint arXiv:2203.13457*, 2022b.

Minghao Xu, Jian Zhang, Bingbing Ni, Teng Li, Chengjie Wang, Qi Tian, and Wenjun Zhang. Adversarial domain adaptation with domain mixup. In *Proceedings of the AAAI Conference on Artificial Intelligence*, volume 34, pp. 6502–6509, 2020.

Xufeng Yao, Yang Bai, Xinyun Zhang, Yuechen Zhang, Qi Sun, Ran Chen, Ruiyu Li, and Bei Yu. Pcl: Proxy-based contrastive learning for domain generalization. In *Proceedings of the IEEE/CVF Conference on Computer Vision and Pattern Recognition*, pp. 7097–7107, 2022.

Kaichao You, Mingsheng Long, Zhangjie Cao, Jianmin Wang, and Michael I. Jordan. Universal domain adaptation. In *IEEE Conference on Computer Vision and Pattern Recognition, CVPR 2019, Long Beach, CA, USA, June 16-20, 2019*, pp. 2720–2729. Computer Vision Foundation / IEEE, 2019.

Marvin Zhang, Henrik Marklund, Abhishek Gupta, Sergey Levine, and Chelsea Finn. Adaptive risk minimization: A meta-learning approach for tackling group shift. *arXiv preprint arXiv:2007.02931*, 8:9, 2020.

Shanshan Zhao, Mingming Gong, Tongliang Liu, Huan Fu, and Dacheng Tao. Domain generalization via entropy regularization. *Advances in Neural Information Processing Systems*, 33: 16096–16107, 2020.

Fan Zhou, Zhuqing Jiang, Changjian Shui, Boyu Wang, and Brahim Chaib-draa. Domain generalization with optimal transport and metric learning. *arXiv preprint arXiv:2007.10573*, 2020a.

Kaiyang Zhou, Yongxin Yang, Timothy Hospedales, and Tao Xiang. Learning to generate novel domains for domain generalization. In *European conference on computer vision*, pp. 561–578. Springer, 2020b.

Kaiyang Zhou, Yongxin Yang, Yu Qiao, and Tao Xiang. Domain generalization with mixstyle. *arXiv preprint arXiv:2104.02008*, 2021.

A Details of experiments

A.1 Experimental Setup

Datasets	# images	# domains	# classes
PACS	9991	4	7
VLCS	10729	4	5
OfficeHome	15588	4	65
TerraIncognita	24788	4	10
DomainNet	586575	6	345

Table 5: Statistics of datasets.

Here we elaborate the detailed experimental setup of our paper. Following DomainBed (Gulrajani & Lopez-Paz, 2020), we split 80%/20% data from source domains as the training/validation set. The best-performing model on the validation set will be evaluated on the testing target domain to obtain the test performance. The statistics of the experimental datasets are shown in Table 5. We list the number of images, domains, classes in each dataset. The proposed model is optimized using Adam (Kingma & Ba, 2015) with the learning rate of 5e-5. The hyper-parameter λ is searched over $\{0.1, 1, 2, 5\}$, and β is tuned in the range of $\{0.01, 0.05, 0.1\}$. The temperature τ is set to 0.1 by default. For the projection head used for contrastive learning, we use a two-layer MLP with ReLU and BatchNorm. Regarding variational reconstruction, following Cha et al. (2022), we employ a simple yet effective architecture, in which the identity function is used as mean encoder and a bias-only network with softplus activation for the variance encoder. More intricate architecture can be explored in the future. Following Gulrajani & Lopez-Paz (2020), for all the datasets except DomainNet, we train the model for 5000 steps. For the DomainNet dataset, we train the model for 15000 steps. Other algorithm-agnostic hyper-parameters such as the batch size are all set to be the same as in the standard benchmark DomainBed (Gulrajani & Lopez-Paz, 2020). For batch construction, we sample the same number of samples from each training domain as in DomainBed (Gulrajani & Lopez-Paz, 2020). Generative Transformation is done for all 4 layers in ResNet-18/50. The experiments are all conducted on one Tesla V100 32 GB GPU. For the data augmentation strategy, previous works usually adopted random cropping, grayscale, horizontal flipping and random color jittering. In this paper, we simply increase the intensity of random color jittering to achieve more aggressive data augmentation. The experimental results have verified the effectiveness of the strategy. Developing stronger and more adaptive augmentation methods for contrastive learning on DG may further enhance the performance.

A.2 Experimental Results on TerraIncognita, VLCS, and DomainNet Data Sets

We put the experimental comparisons with state-of-the-art baselines on TerraIncognita, VLCS, and DomainNet data sets respectively in Tables 6, 7, and 8. The symbol + in the tables is used to denote that the reproduced experimental performance is distinct from the originally reported one such as "PCL$^+$" in Table 8. We can observe our proposed DCCL still surpasses previous methods, which is consistent with the conclusion in the main text and successfully verify the effectiveness of our proposed method.

A.3 Visualization

We demonstrate the embeddings of ERM, PCL, and our DCCL methods on the testing domain in Figure 5. ERM, among the three methods, has the most samples distributed in the central area which cannot be distinguished. For the embedding of contrastive-learning-based baseline PCL, there are fewer samples distributed ambiguously. However, the class clusters are not compact and the class boundaries are not clear. By contrast, our DCCL learns discriminative representations even in the unseen target domain by enhancing intra-class connectivity in CL.

Algorithm	L100	L38	L43	L46	Avg.
MMD (Li et al., 2018b)	41.9	34.8	57.0	35.2	42.2
GroupDRO (Ganin et al., 2016)	41.2	38.6	56.7	36.4	43.2
Mixstyle (Zhou et al., 2021)	54.3	34.1	55.9	31.7	44.0
ARM (Zhang et al., 2020)	49.3	38.3	55.8	38.7	45.5
MTL (Blanchard et al., 2021)	49.3	39.6	55.6	37.8	45.6
CDANN (Li et al., 2018b)	47.0	41.3	54.9	39.8	45.8
VREx (Krueger et al., 2021)	48.2	41.7	56.8	38.7	46.4
RSC (Huang et al., 2020)	50.2	39.2	56.3	40.8	46.6
DANN (Ganin et al., 2016)	51.1	40.6	57.4	37.7	46.7
SelfReg (Kim et al., 2021)	48.8	41.3	57.3	40.6	47.0
IRM (Arjovsky et al., 2019)	54.6	39.8	56.2	39.6	47.6
CORAL (Sun & Saenko, 2016)	51.6	42.2	57.0	39.8	47.7
MLDG (Li et al., 2018a)	54.2	44.3	55.6	36.9	47.8
ERM (Vapnik, 1999)	54.3	42.5	55.6	38.8	47.8
I-Mixup (Xu et al., 2020)	59.6	42.2	55.9	33.9	47.9
SagNet (Nam et al., 2021)	53.0	43.0	57.9	40.4	48.6
COMEN (Chen et al., 2022)	56.0	44.3	58.4	39.4	49.5
SWAD (Cha et al., 2021)	55.4	44.9	59.7	39.9	50.0
PCL (Yao et al., 2022)	58.7	46.3	60.0	43.6	52.1
MIRO (Cha et al., 2022)	60.9	47.6	59.5	43.4	52.9
Ours	**62.2**	**48.3**	**60.6**	**43.6**	$\mathbf{53.7 \pm 0.2}$

Table 6: Experimental comparisons with state-of-the-art methods on TerraIncognita benchmark with ResNet-50.

Algorithm	C	L	S	V	Avg
GroupDRO (Ganin et al., 2016)	97.3	63.4	69.5	76.7	76.7
RSC (Huang et al., 2020)	97.9	62.5	72.3	75.6	77.1
MLDG (Li et al., 2018a)	97.4	65.2	71.0	75.3	77.2
MTL (Blanchard et al., 2021)	97.8	64.3	71.5	75.3	77.2
ERM (Vapnik, 1999)	98.0	64.7	71.4	75.2	77.3
I-Mixup (Xu et al., 2020)	98.3	64.8	72.1	74.3	77.4
MMD (Li et al., 2018b)	97.7	64.0	72.8	75.3	77.5
CDANN (Li et al., 2018b)	97.1	65.1	70.7	77.1	77.5
ARM (Zhang et al., 2020)	98.7	63.6	71.3	76.7	77.6
SagNet (Nam et al., 2021)	97.9	64.5	71.4	77.5	77.8
SelfReg (Kim et al., 2021)	96.7	65.2	73.1	76.2	77.8
Mixstyle (Zhou et al., 2021)	98.6	64.5	72.6	75.7	77.9
PCL (Yao et al., 2022)	99.0	63.6	73.8	75.6	78.0
VREx (Krueger et al., 2021)	98.4	64.4	74.1	76.2	78.3
COMEN (Chen et al., 2022)	98.5	64.1	74.1	77.0	78.4
IRM (Arjovsky et al., 2019)	98.6	64.9	73.4	77.3	78.6
DANN (Ganin et al., 2016)	99.0	65.1	73.1	77.2	78.6
CORAL (Sun & Saenko, 2016)	98.3	**66.1**	73.4	77.5	78.8
SWAD (Cha et al., 2021)	98.8	63.3	75.3	79.2	79.1
MIRO (Cha et al., 2022)	98.8	64.2	75.5	79.9	79.6
Ours	**99.1**	64.0	**76.1**	**80.7**	$\mathbf{80.0 \pm 0.1}$

Table 7: Experimental comparisons with state-of-the-art methods on VLCS benchmark with ResNet-50.

A.4 Representation Connectivity of Pre-Trained Models

Our motivation to utilize pre-trained models for better connectivity is intuitive: we consider pre-trained model can return effective representations modeling the pairwise interactions among images, which thus draws target domains closer to source domains. To verify the motivation, we conduct experiments to evaluate whether the pre-trained model is "well-connected".

1. We design a quantitative **metric to help evaluate** whether the pre-trained space is "well-connected". For images within the same class, we take those images as nodes and construct a graph, only connecting two nodes when their distance on the pre-trained space is smaller than

Algorithm	clip	info	paint	quick	real	sketch	Avg
MMD (Li et al., 2018b)	32.1	11.0	26.8	8.7	32.7	28.9	23.4
GroupDRO (Ganin et al., 2016)	47.2	17.5	33.8	9.3	51.6	40.1	33.3
VREx (Krueger et al., 2021)	47.3	16.0	35.8	10.9	49.6	42.0	33.6
IRM (Arjovsky et al., 2019)	48.5	15.0	38.3	10.9	48.2	42.3	33.9
Mixstyle (Zhou et al., 2021)	51.9	13.3	37.0	12.3	46.1	43.4	34.0
ARM (Zhang et al., 2020)	49.7	16.3	40.9	9.4	53.4	43.5	35.5
CDANN (Li et al., 2018b)	54.6	17.3	43.7	12.1	56.2	45.9	38.3
DANN (Ganin et al., 2016)	53.1	18.3	44.2	11.8	55.5	46.8	38.3
RSC (Huang et al., 2020)	55.0	18.3	44.4	12.2	55.7	47.8	38.9
I-Mixup (Xu et al., 2020)	55.7	18.5	44.3	12.5	55.8	48.2	39.2
SagNet (Nam et al., 2021)	57.7	19.0	45.3	12.7	58.1	48.8	40.3
MTL (Blanchard et al., 2021)	57.9	18.5	46.0	12.5	59.5	49.2	40.6
MLDG (Li et al., 2018a)	59.1	19.1	45.8	13.4	59.6	50.2	41.2
CORAL (Sun & Saenko, 2016)	59.2	19.7	46.6	13.4	59.8	50.1	41.5
SelfReg (Kim et al., 2021)	60.7	21.6	49.4	12.7	60.7	51.7	42.8
MetaReg (Balaji et al., 2018)	59.8	**25.6**	50.2	11.5	64.6	50.1	43.6
DMG (Chattopadhyay et al., 2020)	65.2	22.2	50.0	15.7	59.6	49.0	43.6
ERM (Vapnik, 1999)	63.0	21.2	50.1	13.9	63.7	52.0	44.0
COMEN (Chen et al., 2022)	64.0	21.1	50.2	14.1	63.2	51.8	44.1
PCL$^+$ (Yao et al., 2022)	64.3	20.9	52.7	**16.7**	62.2	55.5	45.4
SWAD (Cha et al., 2021)	66.0	22.4	53.5	16.1	65.8	55.5	46.5
MIRO (Cha et al., 2022)	66.4	23.5	54.1	16.2	66.8	54.8	47.0
Ours	**66.9**	23.0	**55.1**	16.0	**67.7**	**56.1**	$\mathbf{47.5 \pm 0.0}$

Table 8: Experimental comparisons with state-of-the-art methods on DomainNet benchmark with ResNet-50.

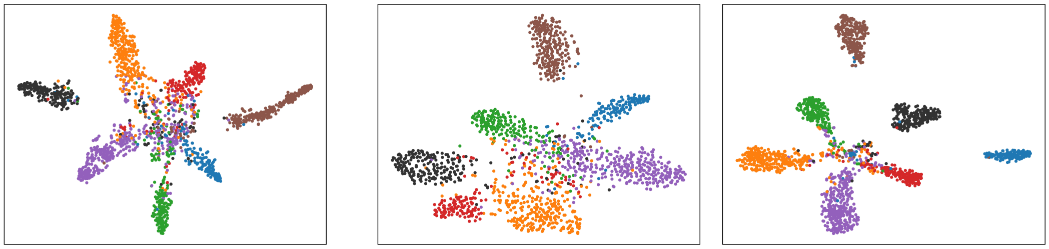

(a) ERM

(b) PCL

(c) DCCL

Figure 5: t-SNE visualization of the ERM, PCL and DCCL representations on the testing domain. Same-class points are in the same colors. We visualize the embedding on PACS dataset where the source domains are photo, sketch, and cartoon; the target domain is art.

a threshold. We denote the smallest possible threshold which makes the graph **connected** as τ, and denote the mean and the std of the pairwise distances respectively as μ and σ. We can thus use $(\tau - \mu)/\sigma$ as a metric to describe the connectivity of the representations.

2. We report the mean (max) metrics (the smaller, the better) of each class for ERM and pre-trained model on PACS, VLCS, and Terra.; the values for ERM are 1.37 (2.68), 1.78 (2.15), and 3.31 (3.56), for pre-trained model 0.54 (0.81), 0.46 (0.62), and 0.63 (0.76). The results confirm the pre-trained space is well-connected.

Furthermore, the variation in performance improvement across different datasets can be attributed to differences in connectivity. We define a measure to evaluate connectivity in Appendix A.4 where lower values indicate better connectivity. For the pre-trained (ERM) model, the connectivity measure we have is 0.54 (1.37) for PACS and 0.49 (2.85) for OfficeHome. A larger discrepancy in connectivity between ERM and the pretraine model ($\frac{1.37}{0.54}$ v.s. $\frac{2.85}{0.49}$) allows for greater potential for improvement.

A.5 Further Ablation Study

Choices of VAE structures. In our experiments, using more advanced VAE structures like HFVAE (Esmaeili et al., 2019) (72.7) and IntroVAE (Huang et al., 2018) (73.1) will yield worse results than vanilla VAE (73.5), which may be attributed to the increased training difficulty.

Choices of contrastive learning methods. SimCLR is denoted as "SelfContrast" in Table 4. Our proposed DCCL (73.5) turns out to outperform other representative SSL approaches: SimCLR (Chen et al., 2020) (68.9 in Tab. 4), MoCo (He et al., 2020) (69.7), BYOL (Grill et al., 2020) (70.7), SwAV (Caron et al., 2020) (71.5).

Further justification of cross-domain contrast (CDC). To further justify cross-domain contrast (CDC), we also implement a baseline using within-domain positive samples only, and the accuracy drops remarkably compared to CDC (71.8 → 70.4). In addition, we include an oracle experiment with solely cross-domain positive pairs and observe comparable performance (71.8 → 71.9). It may require careful design to make good use of domain information to obtain improvements.

Choices of pre-trained backbone and resources. In Table 9, we present additional experiments on Instagram (3.6B) pre-trained RegNet. Compared to PCL, which ignores the pre-trained information, DCCL achieves consistent and substantial improvement on imagenet pre-trained models. And when applied to Instagram, the improvement becomes remarkably larger. These indicate the importance of the pre-trained information, and more abundant the pre-training resources, the stronger the pre-trained information is needed.

Backbone	ResNet-18	ResNet-50	RegNet
Resource	ImageNet (1.3M)		Instagram (3.6B)
PCL	65.0	71.6	73.2
DCCL	**67.5** (+2.5)	**73.5** (+1.9)	**82.5** (+9.3)

Table 9: Perf with different pre-trained resources.

Further Experiments on the Wilds Benchmark.

We also test the OOD performance of our proposed DCCL using the Camelyon and iWildCam datasets from the Wilds benchmark with the pre-trained ResNet-50 network. In Table 10, DCCL demonstrate a consistent and substantial improvement in performance on the more challenging datasets.

Datasets	Camelyon		iWildCam
Metrics	Avg. Acc	Worst Acc	F1
ERM	88.7	68.3	31.3
PCL	91.2	75.5	30.2
DCCL	**96.7**	**90.9**	**32.7**

Table 10: Perf on Wilds datasets with pre-trained ResNet-50.

Further Ablation Study on the VLCS dataset.

Here we additionally performed an ablation study on the VLCS dataset, as shown in Table 11, where the performance gain above SWAD is relatively smaller. These results further confirm that the three components we identified contribute consistently to the effectiveness, as detailed in our paper.

B Related work

In this section, we review the related works in domain generalization and contrastive learning.

B.1 Domain generalization

The goal of DG is to enable models to generalize to unknown target domains under distribution shifts. The related literature can be split into several categories as follows.

Algorithm	C	L	S	V	Avg
SWAD	98.8	63.3	75.3	79.2	79.1
DCCL w/o CDC	98.9	63.8	75.6	79.5	79.4
DCCL w/o PMA	98.6	63.7	75.7	79.3	79.3
DCCL w/o GT	98.7	**64.3**	75.2	80.2	79.6
DCCL	**99.1**	64.0	**76.1**	**80.7**	**80.0**

Table 11: Ablation Study on VLCS dataset with pre-trained ResNet-50.

(i) The first line of work focuses on learning policies. One strategy is meta learning (Finn et al., 2017), which adapts to new environments rapidly with limited observations; the meta-optimization idea was thus introduced in DG (Li et al., 2018a; Balaji et al., 2018; Qiao et al., 2020) to generalize to future testing environments/domains; another widely-studied strategy is ensemble learning (Cha et al., 2021; Chu et al., 2022), claiming DG can benefit from several diverse neural networks to obtain more robust representations. (ii) The second line of work is data augmentation. Many fabricated or learnable augmentation strategies (Volpi et al., 2018; Zhou et al., 2020b; Li et al., 2021; Xu et al., 2020) were developed to regularize and enhance deep learning models. In our paper, we verify more aggressive augmentation can lead to better representations in CL as well. (iii) The last series of work is domain invariant learning. Researchers seek to learn invariances across multiple observed domains for improved generalization on target domains. The commonly used approaches include domain discrepancy regularization (Li et al., 2018b; Zhou et al., 2020a) and domain adversarial learning (Li et al., 2018c; Ganin et al., 2016; Matsuura & Harada, 2020). Recently, MIRO (Cha et al., 2022) began to explore the retention of pre-trained features by designing the mutual information regularization term. The paper (Liu et al., 2023) also utilized the concept connectivity to build up the method. However, their concept of ”connectivity” based on joint distribution clearly differ from our paper. Therefore the theoretical motivation behind two papers are indeed different. Moreover, the methods proposed are different. Except for the common strategy of strong augmentation recommended by the contrastive learning theory paper Wang et al. (2022b), our proposed methods are different from the ones in Liu et al. (2023). They propose two nearest-neighbor-based methods for constructing positive pairs, while our main contribution lies in the exploitation of both the pre-trained models and the intra-class data connectivity.

B.2 Contrastive learning

Contrastive learning (CL) (Chen et al., 2020) aims to learn discriminative sample representation by aligning positive instances and pushing negative ones apart. As a promising self-supervised learning paradigm, CL is widely used in unsupervised pre-training to improve the performance of downstream tasks (Hjelm et al., 2019; Gao et al., 2021; Li et al., 2022; He et al., 2020; Chen et al., 2020; Caron et al., 2020; Chen & He, 2021; Grill et al., 2020). SimCLR (Chen et al., 2020) is the CL framework that first reveals the projection head and data augmentation as the core components to learn invariant representation across views. MoCo (He et al., 2020) proposes to build a dynamic queue dictionary to enlarge batch size for effective learning. There are also works (Khosla et al., 2020; Gunel et al., 2020; Cui et al., 2021) adapting CL to the supervised setting to leverage label information.

The capability of CL to obtain class-separated representations has also motivated the application in domain generalization. SelfReg (Kim et al., 2021) introduced a new regularization method to build self-supervised signals with only positive samples; PCL (Yao et al., 2022) proposed a proxy-based approach to alleviate the positive alignment issue in CL; COMEN (Chen et al., 2022) used a prototype-based CL component to learn the relationships between various hidden clusters. However, the role of CL in domain generalization is not yet well explored, and our work is dedicated to shedding some light on the understanding of its effect from a intra-class connectivity perspective.

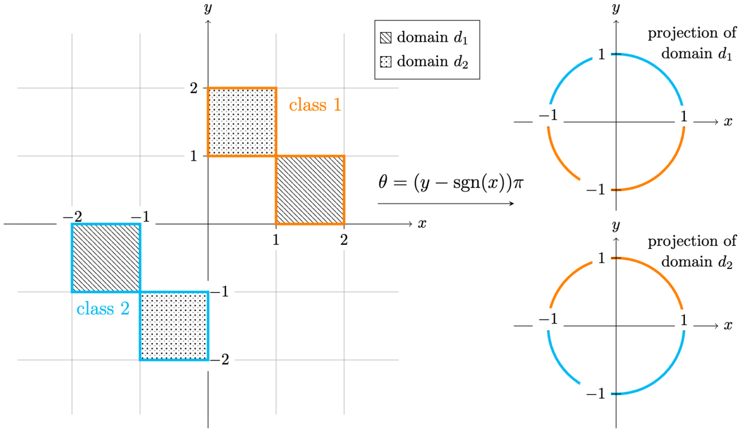
y
x
2
1
−2
−1
1
2
−1
−2
class 1
class 2
▨ domain d_1
⬚ domain d_2
$\theta = (y - \mathrm{sgn}(x))\pi$
projection of domain d_1
projection of domain d_2
1
−1

Figure 6: Illustration for the toy example of self-contrastive learning (SCL). Spots and slashes are filled in to represent different domains; orange and blue rectangles respectively denote classes 1 and 2. The mapping function $\varphi \circ \theta$ learned on domain d_1 can perfectly classify the samples, and the mapping attains perfect alignment and uniformity (the objective of SCL). However, when applied to a new domain d_2, the classifier completely fails (0% acc).

C Failure of self-contrastive learning in domain generalization

Self-contrastive learning, which aligns the augmentation views of the same input, has achieved successful performance in unsupervised pre-training tasks (Chen et al., 2020; He et al., 2020; Grill et al., 2020). However, it does not naturally fit the domain generalization setting since it assumes the ability to sample x from the whole data distribution; in the training stage of domain generalization, we instead are only able to access partial domains. This mismatch can lead to suboptimal performance in domain generalization if the users mechanically adopt the classical contrastive learning loss.

We provide a linearly separable toy example in Figure 6 to show the deficiency of SCL that even attaining optimal CL loss (1) cannot guarantee good performance in the domain generalization setting, where only partial domains are involved in the training. In the figure, slashes and spots are used to represent domains d_1 and d_2; orange and blue rectangles respectively denote classes 1 and 2. We specifically consider the extreme case that **no** augmentation is applied and only domain d_1 is involved in the training. We then construct a map $\varphi(\theta(x)) := (\cos(\theta), \sin(\theta))$ with $\theta(x) = (x - \mathrm{sgn}(y))\,\pi$ [5]. The map $f_h = \varphi \circ \theta$ attains perfect alignment (due to no augmentation) and maximal uniformity (new representations are uniformly distributed on the corresponding circle arcs) on the 1-sphere $\mathbb{S}^1 := \left\{x \in \mathbb{R}^2 : \|x\|_2 = 1\right\}$, and based on the derivation in Wang & Isola (2020) f_h will minimize the CL loss (1). However, the new representations for domain d_2 do not reflect the class information and even have the opposite signs as domain d_1.

We can conclude that the usage of classical SCL does not necessarily lead to good performance under the domain generalization setting; and empirical verification is provided in Section 4.4 as well. Similar limitation is observed in invariance-based DG methods (Shui et al., 2022). We provide the detailed settings of the coined data distribution as follows.

Example C.1 (Self-contrastive learning does not help domain generalization.)**.** *Let the label collection $\mathcal{Y}$ be $\{-1, 1\}$ and the portions of two classes are both* 0.5*. Assume there are two domains d_1 and d_2: if a sample $X = (X_1, X_2) \in \mathbb{R}^2$ with label Y is from domain d_1, its conditional distribution will be specified as*

$$\begin{cases} X_1 \sim \mathrm{Unif}\,(0,1)\,Y, \\ X_2 \sim \mathrm{Unif}\,(1,2)\,Y, \\ X_1 \perp\!\!\!\perp X_2 \mid Y; \end{cases}$$

in domain d_2 the distribution of X_1, X_2 is interchanged. Considering the extreme case that ***no*** *augmentation is applied and only domain d_1 is involved in the training, we construct a map*

[5] $\mathrm{sgn}(y) := \mathbf{1}_{\{y \geq 0\}} - \mathbf{1}_{\{y<0\}}$ is the sign function.

$\varphi(\theta(x)) := (\cos(\theta), \sin(\theta))$ *with* $\theta(x) = (x_1 - \operatorname{sgn}(y))\,\pi$ [6]. *The map* $f_h = \varphi \circ \theta$ *attains perfect alignment (due to no augmentation) and maximal uniformity (new representations are uniformly distributed on the corresponding circle arcs) on the* 1*-sphere* $\mathbb{S}^1 := \left\{x \in \mathbb{R}^2 : \|x\|_2 = 1\right\}$*, and based on the derivation in Wang & Isola (2020)* f_h *will minimize the CL loss (1). However, the new representations for domain* d_2 *do not reflect the class information and even have the opposite signs as domain* d_1*.*

SCL in the previous example fails to obtain **intra-class connectivity** due to insufficient data augmentation and domain-separated (rather than class-separated) representations, which ultimately causes poor generalization performance. Inspired by the above analysis, we thus propose two approaches to improve intra-class connectivity: (i) applying more aggressive data augmentation and (ii) expanding the scope of positive samples, from solely self-augmented outputs $a(x)$ to the augmentation of intra-class samples across domains.

D Discussions & Limitations

In the paper, We analyze the failure of directly applying SCL to DG with the CL theory and suggest lack of intra-class connectivity in the DG setting causes the deficiency. We accordingly propose domain-connecting contrastive learning (DCCL) to enhance the connectivity across domains and obtain generalizable and transferable representation for DG. Extensive experiments also verify the effectiveness of our method.

However, we're also aware of the **limitations** of our work. We don't make explicit use of the domain information. It implies if one can well leverage the domain information, better generalization performance might be obtained. Moreover, similar to Cha et al. (2022), our proposed DCCL requires the pre-trained embeddings of the samples. This existing drawback can be mitigated by generating the pre-trained embeddings in advance and storing them locally. In addition, how to develop stronger and more adaptive augmentation methods for contrastive learning on DG is not explored in this paper and remains an open problem.

Regarding **attribution of existing assets**, we only utilize existing open-sourced datasets, which all can be found in DomainBed[7] benchmark. In addition, we don't make any use of **personal data**. For all the datasets used, there is no private personally identifiable information or offensive content.

[6] $\operatorname{sgn}(y) := \mathbf{1}_{\{y \geq 0\}} - \mathbf{1}_{\{y<0\}}$ is the sign function.

[7] https://github.com/facebookresearch/DomainBed